

Proton decay of $T_{>}$ hole states in heavy nuclei by means of the $({}^3\text{He}, \alpha p)$ reaction on ${}^{96}\text{Zr}$ and ${}^{144}\text{Sm}$

S. Galès, Y. El Hage, S. Fortier, H. Laurent, J. M. Maison, and J. P. Schapira
Institut de Physique Nucléaire, BP No. 1, 91406 Orsay, France

J. L. Foster, Jr.
Universidade de São Paulo, Instituto de Física, São Paulo, Brasil
 (Received 28 October 1977)

The ${}^{96}\text{Zr}({}^3\text{He}, \alpha p){}^{94}\text{Y}$ and the ${}^{144}\text{Sm}({}^3\text{He}, \alpha p){}^{142}\text{Pm}$ reactions studied at 39 MeV incident energy were used to investigate the proton decay of hole analog states. The α particles leading to these unbound levels in ${}^{95}\text{Zr}$ and ${}^{143}\text{Sm}$ were detected near 0° in coincidence with the protons emitted from the $T_{>}$ hole states. In the case of the $2d_{5/2}$ hole analog state in ${}^{143}\text{Sm}$ only a mean value for the proton branching ratio has been determined from this study. Proton hole-neutron hole states have been observed in ${}^{94}\text{Y}$ through the proton decay of the $2p_{1/2}$, $2p_{3/2}$, and $1f_{5/2}$ $T_{>}$ levels of ${}^{95}\text{Zr}$. Analysis of the α - p angular correlations has given inelastic proton widths, spins, and parities as well as shell model configurations of several of the observed residual states in ${}^{94}\text{Y}$.

[NUCLEAR REACTIONS ${}^{96}\text{Zr}({}^3\text{He}, \alpha p)$, ${}^{144}\text{Sm}({}^3\text{He}, \alpha p)$, $E = 39$ MeV; measured $\sigma(E_\alpha, E_p, \theta_p)$. ${}^{95}\text{Zr}$, ${}^{143}\text{Sm}$ deduced IAS, proton branching. ${}^{94}\text{Y}$ deduced levels, J, π, Γ_p , spectroscopic factors. Enriched targets. 0° spectrometer.]

I. INTRODUCTION

Previous studies of the particle decay of isobaric analog states (IAS) have dealt mainly with those analog states formed in the proton resonant elastic and inelastic reactions.¹ It has been shown that these experiments provide quantitative informations on the shell model configurations of the neutron particle-hole states of the core C , selectively populated in the inelastic channel. However until recently, no extensive studies have been reported on $T_{>}$ hole states²⁻⁴ in heavy nuclei ($A \geq 100$) and no experiments have been reported on their particle decay. To show the interest of such an investigation, we consider a parent level formed by the coupling of a proton hole p_j^{-1} to a doubly closed shell core C . The wave function of its analog state consists of two terms, shown schematically in Fig. 1. Such $T_{>}$ hole states could be populated through neutron pickup experiments [e.g., $({}^3\text{He}, \alpha)$, (p, d) , etc.] as illustrated by the term $n_j^{-1} \otimes C$ of their wave function. In the case of heavy nuclei with a large neutron excess, the IAS is unbound with re-

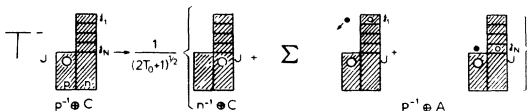


FIG. 1. Schematic representation of the shell model structure of a proton-hole state and its analog state in heavy nuclei.

spect to the particle decay channel and can therefore decay by the emission of a proton \tilde{p}_j (see Fig. 1). This leads to the population of hole-hole multiplets $[(J)_p^{-1} \otimes (j)_n^{-1}]$ in the residual nuclei.

The motivation of this paper is to show that it is possible through the study of the $({}^3\text{He}, \alpha \tilde{p})$ process in a suitable geometry, not only to identify these levels but also to extract quantitative informations about their spins and parities and their configurations. In our recent study of the ${}^{96}\text{Zr}({}^3\text{He}, \alpha){}^{95}\text{Zr}$ reaction,⁵ total widths, angular momentum transfers, and spectroscopic factors have been deduced for the $2p_{1/2}$ ($E_x = 14.98$ MeV), $2p_{3/2}$ ($E_x = 15.64$ MeV), and $1f_{5/2}$ ($E_x = 15.79$ MeV) IAS in ${}^{95}\text{Zr}$. No information was available about the $T_{>}$ hole states in ${}^{143}\text{Sm}$ before the present work.

II. EXPERIMENTAL PROCEDURE AND RESULTS

The ${}^{96}\text{Zr}({}^3\text{He}, \alpha \tilde{p}){}^{94}\text{Y}$ and ${}^{144}\text{Sm}({}^3\text{He}, \alpha \tilde{p}){}^{142}\text{Pm}$ reactions have been investigated with the Orsay MP tandem accelerator at 39 MeV incident energy. The experimental setup for the angular correlation data has been described in detail in our previous reports⁶ and will be discussed only briefly in this paper.

The targets consisted of self-supporting metal foils, enriched in ${}^{96}\text{Zr}$ (72%) and ${}^{144}\text{Sm}$ (97%) with a thickness of about $600 \mu\text{g}/\text{cm}^2$. The α particles were detected near 0° with a triplet of magnetic quadrupole lenses.⁷ Reaction products were focused onto a 300 mm^2 , $700 \mu\text{m}$ thick Si detector.

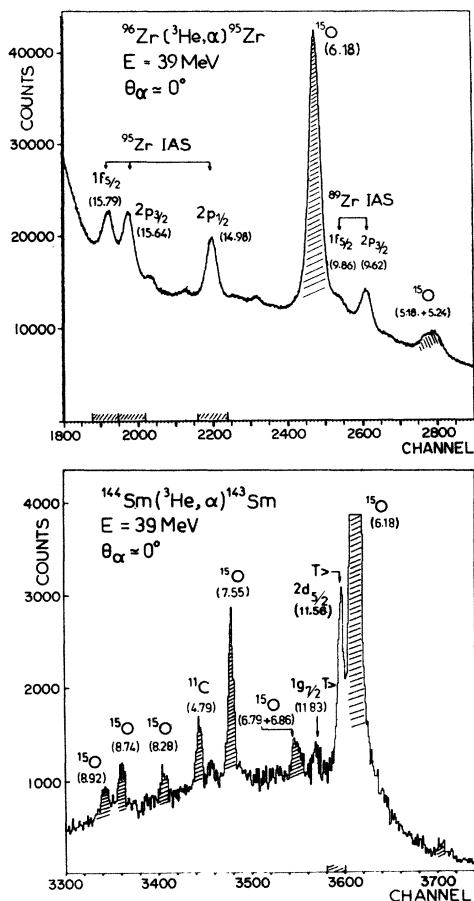


FIG. 2. Single α particle energy spectra from the ${}^{96}\text{Zr}({}^3\text{He}, \alpha){}^{95}\text{Zr}$ and the ${}^{144}\text{Sm}({}^3\text{He}, \alpha){}^{143}\text{Sm}$ reactions taken with the 0° spectrometer. Excitation energies of IAS in ${}^{95}\text{Zr}$, ${}^{89}\text{Zr}$, and ${}^{143}\text{Sm}$ are indicated in the figure. The dashed part of the x axis in the two spectra represents the window taken in the energy spectra to build the coincident proton decay of these IAS.

The coincident protons were detected in eight $1500\ \mu\text{m}$ thick Si(Li) counters placed on a turnable plate in a scattering chamber. Coincidence events were measured for proton lab angles ranging from 85° to 163° by typically 12° steps. The procedure adopted for absolute normalization of the angular correlation as well as for the data reduction were the same as in Ref. 6. The direct α spectra obtained for the reactions ${}^{96}\text{Zr}({}^3\text{He}, \alpha){}^{95}\text{Zr}$ and ${}^{144}\text{Sm}({}^3\text{He}, \alpha){}^{143}\text{Sm}$ are presented in Fig. 2. The overall energy resolution obtained in these spectra was about $50\ \text{keV}$ (full width at half maximum). Besides the contaminant α groups from neutron pickup on light nuclei (${}^{12}\text{C}$, ${}^{16}\text{O}$), a number of narrow lines are clearly present in the two spectra of Fig. 2. In the case of the ${}^{96}\text{Zr}$ target (upper part of Fig. 2) three levels in ${}^{95}\text{Zr}$ are observed

with excitation energies in close agreement with those determined in our recent study of the ${}^{96}\text{Zr}({}^3\text{He}, \alpha){}^{95}\text{Zr}$ reaction.⁵ They were identified as the IAS of the $2p_{1/2}$, $2p_{3/2}$, and $1f_{5/2}$ levels of the ${}^{95}\text{Y}$ parent nucleus.⁵ In addition, two peaks originating from the ${}^{90}\text{Zr}({}^3\text{He}, \alpha){}^{89}\text{Zr}$ reaction are also present due to the isotopic abundance of the ${}^{90}\text{Zr}$ nuclei in the target (14%) and they were assigned as the $2p_{3/2}$ and $1f_{5/2}$ IAS in ${}^{89}\text{Zr}$. The deduced yields of the IAS in ${}^{95}\text{Zr}$ are found large enough ($d\sigma/d\Omega = 500$ to $200\ \mu\text{b}/\text{sr}$ at $\theta = 0^\circ$) to allow the investigation in coincidence of their proton decay. For the ${}^{144}\text{Sm}$ target, the magnetic field in the 0° spectrometer was set in order to obtain the maximum solid angle ($\Omega \approx 10\ \text{msr}$) for α particles leading to an excitation energy about $11.5\ \text{MeV}$ in ${}^{143}\text{Sm}$. In this region where one expects the IAS of the ground and first excited states of the ${}^{143}\text{Pm}$ parent nucleus, we clearly observe two narrow lines at excitation energies of, respectively, 11.56 and $11.83\ \text{MeV}$ in ${}^{143}\text{Sm}$ (see the lower part of Fig. 2). This result, together with the spacing and relative yield of these two levels, is consistent with a tentative identification of these lines as the IAS of the $E_x = 0.0$ and $E_x = 0.27\ \text{MeV}$ levels of ${}^{143}\text{Pm}$.⁸ They contain, respectively, a large amount of the $2d_{5/2}$ and $1g_{7/2}$ proton hole strengths in the ${}^{143}\text{Pm}$ nucleus. This evidence was confirmed by data taken at forward angles (10° and 20° lab angles) using a split-pole spectrograph. In this later experiment, an upper limit of $40\ \text{keV}$ has been estimated for the total width of the $11.56\ \text{MeV}$ level in ${}^{143}\text{Sm}$. From the split-pole data the deduced cross sections were found to be, respectively, of $80\ \mu\text{b}/\text{sr}$ for the $2d_{5/2}$ IAS and $10\ \mu\text{b}/\text{sr}$ for the $1g_{7/2}$ IAS at forward angles ($\theta = 10^\circ$), which is considerably lower than the ones obtained for the IAS in ${}^{95}\text{Zr}$.

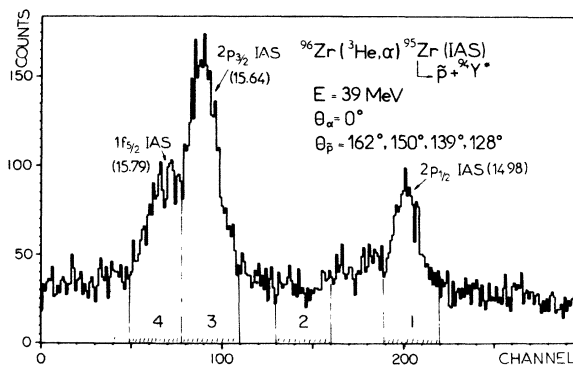


FIG. 3. Coincident α energy spectrum from the ${}^{96}\text{Zr}({}^3\text{He}, \alpha){}^{95}\text{Zr}$ reaction summed over the four proton angles. The numbers 1 to 4 indicated above the dashed portion of the x axis have the same meaning as the one mentioned in the caption of Fig. 2.

Finally, if we consider the two dimensional matrices ($E_\alpha - E_{\tilde{p}}$) built for each proton lab angle, the coincidence events are located along the kinematic lines of the $A(^3\text{He}, \alpha\tilde{p})B$ reaction leading to the different residual states in the nucleus B . The projection of such lines along the α axis produces a coincident α spectrum presented in Fig. 3 in the case of the $^{96}\text{Zr}(^3\text{He}, \alpha\tilde{p})^{94}\text{Y}$ reaction. Two interesting features already appear in this spectrum. (i) The peak to background ratio in Fig. 3 is larger than the one observed in the direct spectrum of Fig. 2. This indicates that the high background observed in the reaction $^{96}\text{Zr}(^3\text{He}, \alpha)^{95}\text{Zr}$ around 15 MeV excitation energy is due mainly to the high density of T_ζ states which decay predominantly by neutron emission and thus is absent in the coincidence yield.

(ii) In Fig. 3 the coincidence yield of the $1f_{5/2}$ IAS seems to be reduced considerably as compared to the observed population of this level in the direct spectra of Fig. 2. On the basis of this comparison, the proton branching ratio of the $2p_{3/2}$ IAS is much larger than the $1f_{5/2}$ one.

III. ANALYSIS OF THE ANGULAR CORRELATION DATA

The method and the formalism of the particle-particle angular correlation used in this analysis are the same as the one used in our previous studies⁶ of the proton decay of unbound states. Only the main formulation and results of that method will be presented here.

A. General

The angular correlation of the emitted proton measured in coincidence in the $(^3\text{He}, \alpha\tilde{p})$ reaction using method II of Litherland and Ferguson⁹ can be deduced from the expression

$$N_I(\theta) = N_\alpha(0^\circ)(\Omega_p/4\pi)[\tilde{\Gamma}_p(I)/\Gamma]W(\theta),$$

with N_I the number of coincident protons emitted at an angle θ , $N_\alpha(0^\circ)$ the number of single α particles detected near 0° , Ω_p the solid angle of the proton detector, and $\tilde{\Gamma}_p(I)$, Γ being, respectively, the proton partial width via channel I and the total width of the IAS. In this geometry, the proton branching ratio $\tilde{\Gamma}_p(I)/\Gamma$ is directly proportional⁶ to the A_0 coefficient of the angular correlation

$$W(\theta) = \sum_{k(\text{even})} A_k P_k(\cos\theta).$$

The A_k coefficients are related to the proton partial widths⁶ in the channel I , $\Gamma_p^{lj}(I)$, where lj are the quantum numbers of the emitted proton and I the spin of the residual state. Therefore from the measured total widths of the IAS,⁵ the total inelas-

tic proton widths have been deduced for each level. The angular correlations were fitted by means of the computer code GRILLE3.⁶

B. Proton branching ratios

1. $^{144}\text{Sm}(^3\text{He}, \alpha\tilde{p})^{142}\text{Pm}$ reaction

In Fig. 4 is displayed a summed coincidence proton spectrum associated with the decay of the $2d_{5/2}$ IAS in ^{143}Sm . The very low statistics obtained in this case for the decay to the various levels of the ^{142}Pm nucleus have permitted one only to deduce a mean value for the proton branching ratio of the 11.56 MeV IAS in ^{143}Sm ; the results are displayed in Table I. The known spectroscopic properties of the low-lying states in the odd-odd ^{142}Pm nucleus are very limited.¹⁰ On that basis the $d_{5/2}$ IAS decay seems to populate selectively the $E_x = 0.25$ MeV level in ^{142}Pm , whereas the feeding of the $E_x = 0.0$ or 0.03 MeV states and the $E_x = 0.45$ MeV level should be considered tentative due to the very low statistics in the coincidence proton spectrum (see Fig. 4). In the framework of the simple model displayed in Fig. 1, one expects to populate the multiplet of states $(d_{5/2})^{-1}_p \otimes [(d_{3/2})^{-1}_n + (s_{1/2})^{-1}_n]$ and therefore the 0.25 MeV state in ^{142}Pm should have a large part of its wave function represented by such configurations.

An interesting comparison can be made between the total inelastic widths measured either in the decay of the hole analog states to the various members of the proton-hole-neutron-hole multiplet or in the proton emission of isobaric analog resonances (IAR) to the neutron-particle-hole states

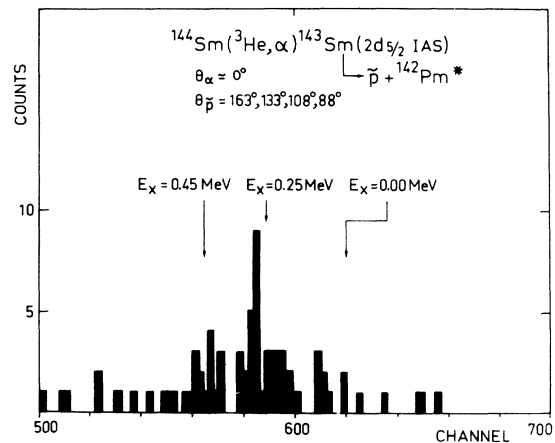


FIG. 4. Summed proton coincidence spectrum for the $^{144}\text{Sm}(^3\text{He}, \alpha)^{143}\text{Sm}(2d_{5/2} \text{ IAS}) \rightarrow p + ^{142}\text{Pm}$ process. The arrows indicate the expected position of the known low-lying levels in the ^{142}Pm nucleus.

TABLE I. Summary of the results from the $^{144}\text{Sm}(^3\text{He}, \alpha\tilde{p})$ reaction.

E_x (IAS) (MeV)	E_x (parent) ^a (MeV)	LJ ^a	Γ (keV)	$\sum \Gamma_p/\Gamma$
11.56 ± 0.03	0.00	$d_{5/2}$	<40	0.08 ± 0.04
11.83 ± 0.03	0.27	$g_{7/2}$

^aReference 8.

of the target nucleus through (p, p') experiments. In the case of a ^{144}Sm target, these configurations are reached through the creation of a particle-hole pair in core state with the same quantum number lj (see Fig. 1). As the total inelastic widths are dominated by the angular momentum l of the emitted proton and the energy available in the decay, when these two quantities are comparable, the total inelastic widths obtained for the hole analog state or the IAR should be nearly equal. This is the case for the $2f_{7/2}$ IAR in ^{145}Eu located at $E_x = 12.57$ MeV and which decays to neutron-particle-hole states centered around 3.7 MeV in ^{144}Sm .¹¹ The sum of the inelastic widths to these particular states was found to be $\sum \Gamma_p = 3.2$ keV.¹¹ For a total width of 45 keV in the case of the $2f_{7/2}$ IAR in ^{145}Eu ¹¹ this leads to a proton branching ratio for the inelastic decay to neutron p-h states of $\sum \Gamma_p/\Gamma = 0.08$. In the case of the $2d_{5/2}$ hole analog located at 11.56 MeV excitation energy in ^{143}Sm and for which the proton decay energy is quite comparable ($E_p = 5, 6$ MeV) we found a mean value for that branching ratio of $\sum \Gamma_p/\Gamma = 0.08 \pm 0.04$ which is in close agreement with the deduced one from the (p, p') study on IAR.

2. $^{96}\text{Zr}(^3\text{He}, \alpha\tilde{p})^{94}\text{Y}$ reaction

The data obtained for the proton decay of the $2p_{1/2}$, $2p_{3/2}$, and $1f_{5/2}$ IAS in ^{95}Zr are presented in Fig. 5. The residual states of ^{94}Y populated in this reaction have been generally observed in a previous study of the $^{96}\text{Zr}(d, \alpha)^{94}\text{Y}$ reaction,^{12,13} but in this nucleus, only the ground state has a well established spin and parity $J^\pi = 2^-$.^{12,13} Following the

TABLE II. Quantum numbers, proton branching ratios, total and inelastic partial widths for IAS in ^{95}Zr .

E_x (IAS) (MeV)	LJ	$\sum \Gamma_p/\Gamma$	Γ ^a (keV)	$\sum \Gamma_p$ (keV)
14.98	$p_{1/2}$	0.21 ± 0.03	32 ± 10	7 ± 3
15.64	$p_{3/2}$	0.36 ± 0.05	70 ± 10	25 ± 7
15.79	$f_{5/2}$	0.19 ± 0.03	55 ± 10	10 ± 3

^aReference 5.

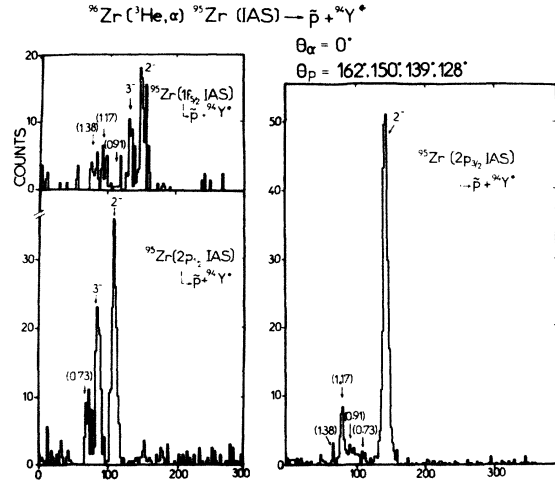


FIG. 5. Summed proton coincidence spectra displaying the proton decay of the IAS in ^{95}Zr . Numbers in parentheses indicate the excitation energy of final states in ^{94}Y populated in the $^{96}\text{Zr}(^3\text{He}, \alpha\tilde{p})^{94}\text{Y}$ reaction.

simple model presented in the Introduction we expect in this case to populate proton-neutron-hole multiplets in ^{94}Y which have the following configurations. The proton hole is a level below $N=40$ with the same quantum number LJ as those of the IAS ($2p_{1/2}$, $2p_{3/2}$, $1f_{5/2}$). The neutron hole is a level below $N=56$ ($2d_{5/2}$, $1g_{9/2}$). The possibility of $g_{9/2}$ hole states will be ignored in the present analysis because of the low $l=4$ penetrability factor for a proton energy of about 4–5 MeV. Therefore the $p_{1/2}$ IAS should populate a $J^\pi = 2^-, 3^-$ doublet of states $[(2p_{1/2})^{-1}_p(2d_{5/2})^{-1}_n]_{2^-, 3^-}$ and similarly $J^\pi = 1^-$ to 4^- and $J^\pi = 0^-$ to 5^- multiplets at higher excitation energies in ^{94}Y should be observed in the decay of the $2p_{3/2}$ and $1f_{5/2}$ IAS. As shown in Fig. 5 the experiment is complicated more by both neutron and proton configuration mixing in the final states. For example, we observe the population of an additional level at 0.73 MeV for the $p_{1/2}$ IAS decay (see Fig. 5) and the states at $E_x = 0.91, 1.17,$ and 1.38 MeV are present in both the $p_{3/2}$ and $f_{5/2}$ decays. In Table II, we report for each IAS, the measured proton branching ratios and the total inelastic widths. We see that the branching ratios are less than unity here also which is consistent with the large neutron energy ($E_n > 8.5$ MeV) available for that channel.

C. Spin assignments and spectroscopic factors for levels in ^{94}Y

To go further in the description of the final states in ^{94}Y populated through the proton emission of the IAS in ^{95}Zr , the angular correlations obtained for each analog state decay were analyzed by a least-

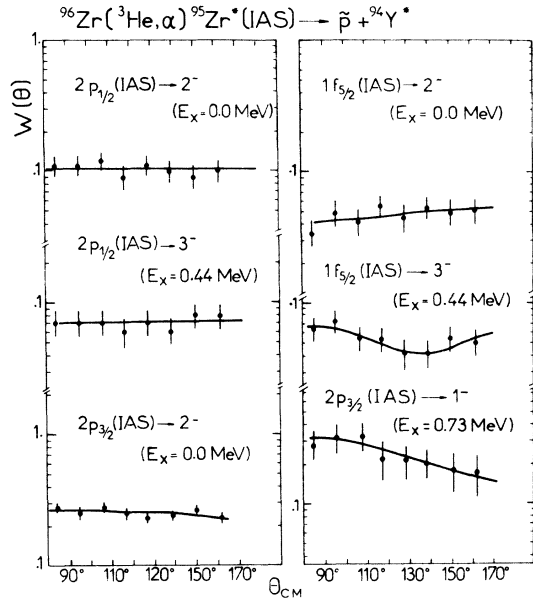


FIG. 6. Angular correlation data for the $^{96}\text{Zr}(^3\text{He}, \alpha)^{95}\text{Zr}^*(\text{IAS}) \rightarrow \bar{p} + ^{94}\text{Y}^*$ reaction. The solid lines represent the obtained fits for the indicated J values and spectroscopic factors of Table III.

squares-fitting procedure. The only free parameters in the analysis of a given transition between the IAS of spin J and a given final state I is the proton partial width $\Gamma_p^{IJ}(I)$ for the $2d_{5/2}$ and $3s_{1/2}$ waves. Although the $3s_{1/2}$ states are above the $N = 56$ subshell, they were introduced in the analysis due to a small occupation of the $3s_{1/2}$ orbital in

^{96}Zr (Ref. 5) and the large difference in the penetrability factor which greatly favors the $l=0$ decay. Some of the data together with the obtained theoretical curves are displayed in Fig. 6. Finally, in order to calculate spectroscopic factors, the single-particle widths Γ_{sp}^{IJ} corresponding to the observed transitions were calculated using the code GAMOV.¹⁴ The proton spectroscopic factors were evaluated from

$$S^{LJ}(j) = \frac{\Gamma_p^{IJ}(I) 2J+1}{\Gamma_{sp}^{IJ}(I) 2I+1}.$$

The resulting values of the spins and spectroscopic factors of the various levels in ^{94}Y are presented in Table III where E_x is the excitation energy of the final state. Entries under I^π are the possible spins of these levels compatible with the experimental correlations. The values of I^π used in the calculations are underlined. When one or more values of I^π are listed in parentheses this indicates that arguments related to the deduced spectroscopic factors are also used and this will be discussed below. The quantities $S^{LJ}(\frac{5}{2})$ and $S^{LJ}(\frac{1}{2})$ are the spectroscopic factors defined above. Our results are now presented for each final state in ^{94}Y .

1. Ground state of ^{94}Y

This level is populated by the decay of the three IAS's studied in this work. In the case of the $p_{1/2}$ IAS, the spin of this state is limited to the possible values $I^\pi = 0^-, 1^-, 2^-, 3^-$. In a model-independent analysis the spins $I=0, 3$ are excluded from the

TABLE III. Spins, spectroscopic factors, and hole-hole configurations of final states in ^{94}Y .

E_x (MeV)	I^π	Main configuration	$S^{LJ}(\frac{5}{2})$	$S^{LJ}(\frac{1}{2})$
0.00	<u>2⁻</u>	$p_{1/2}d_{5/2}$ $p_{3/2}s_{1/2}$ $f_{5/2}s_{1/2}$	0.66	0.39 0.06
0.44	(<u>3⁻</u>)	$p_{1/2}d_{5/2}$ $f_{5/2}s_{1/2}$	0.90	0.11
0.73	(<u>1⁻</u>)	$p_{1/2}s_{1/2}$ $p_{3/2}d_{5/2} + p_{3/2}s_{1/2}$	0.10	0.33 0.17
0.91	(2 ⁻ , 3 ⁻)	Multiple solutions		
1.17	<u>2⁻</u>	$p_{3/2}d_{5/2} + p_{3/2}s_{1/2}$ $f_{5/2}d_{5/2} + f_{5/2}s_{1/2}$	0.15 0.20	0.60 0.35
1.38	(2 ⁻ , 3 ⁻ , 4 ⁻)	Multiple solutions		

measured angular correlation in the $2p_{3/2}$ decay, whereas the spin $I=1$ is inconsistent with our results for the $1f_{5/2}$ decay. Therefore the ground state has a spin and parity $J^{\pi}=2^{-}$ with a large $(p_{1/2})^{-1}_{p}(d_{5/2})^{-1}_{n}$ component in its wave function (see Table III).

2. $E_x = 0.44$ MeV level

Again the $p_{1/2}$ decay limits the spin of this level to $I=0^{-}, 1^{-}, 2^{-}, 3^{-}$. In the limits of our experiment this state is not populated by the proton emission of the $p_{3/2}$ IAS. The angular correlation measured on the $f_{5/2}$ IAS leads to the spin values $I=2, 3$ for this state. The $J^{\pi}=2^{-}$ assumption gives therefore a spectroscopic factor $S^{1,1/2}(\frac{5}{2})=1.3$. The summed value of the $S^{1,1/2}(\frac{5}{2})$ spectroscopic factors for the two first states of ^{94}Y give a too large result (2.0) as compared with the sum rule $\sum_I S^{1,1/2}(\frac{5}{2}) \leq 1$ where the sum is extended for a given IAS over all states of same spin and parity I . On this basis, the spin and parity $J^{\pi}=3^{-}$ is proposed here for this level. The ground and first excited states in ^{94}Y are thus confirmed here as the main components of the $(p_{1/2})^{-1}_{p}(d_{5/2})^{-1}_{n}$ configurations in ^{94}Y .

3. $E_x = 0.73$ MeV level

This state is populated only in the decay of the $p_{1/2}$ and $p_{3/2}$ IAS. The analysis of the data on the $p_{3/2}$ IAS limits the spin of this level to $I=1, 2$. The $J^{\pi}=2^{-}$ assumption again gives too large a spectroscopic factor as compared to the sum rule defined above and therefore the spin and parity $J^{\pi}=1^{-}$ is proposed here for this state. We suggest that this level is one member of the $p_{1/2}s_{1/2}$ multiplet in ^{94}Y (see Table III).

4. 0.91 MeV level

This level is very weakly populated in the $p_{3/2}$ and $f_{5/2}$ IAS decay ($\Gamma_p/\Gamma < 0.03$). Due to the low statistics accumulated in this case only a tentative spin assignment $J^{\pi}=2^{-}, 3^{-}$ could be proposed for this level. The deduced spectroscopic strengths are also rather small and no definite shell model configurations could be suggested in this case.

5. 1.17 MeV level

This level is rather strongly populated in the $^{96}\text{Zr}(d, \alpha)^{94}\text{Y}$ reaction¹² and was proposed as a member of the $(p_{3/2})^{-1}_{p}(d_{5/2})^{-1}_{n}$ multiplet in ^{94}Y . In the $p_{3/2}$ IAS decay, the analysis limits the spin of this state to $I=1, 2$ and the angular correlation measured on the $1f_{5/2}$ hole analog is consistent only with $I=2, 3$. Therefore our study has estab-

lished the spin and parity $J^{\pi}=2^{-}$ for this state. The deduced components of its wave function indicates a large admixture of the $(p_{3/2})^{-1}_{p}[(d_{5/2})^{-1}_{n} + (s_{1/2})^{-1}_{n}]$ and $(f_{5/2})^{-1}_{p}[(d_{5/2})^{-1}_{n} + (s_{1/2})^{-1}_{n}]$ configurations.

6. 1.38 MeV level

This state is only clearly present in the $f_{5/2}$ IAS decay and therefore the possible values for its spin and parity are $I^{\pi}=2^{-}, 3^{-}$, or 4^{-} . From our results no definite configuration could be proposed for the 1.38 MeV level although it is strongly excited in the $^{96}\text{Zr}(d, \alpha)^{94}\text{Y}$ reaction.¹²

A more general comment could be made about the amount of the $2d_{5/2}$ hole strength observed in this experiment. For each final state the sum of the $S^{LJ}(j)$ value is consistent with unity within the experimental errors (20 to 40%). For a given IAS the sum of the spectroscopic factors $S^{LJ}(j)$ extended over all the residual states of spin I populated by a lj proton wave obeys the relation $\sum_I S^{LJ}(j) = 2j + 1$. This sum rule measures the amount of the $2d_{5/2}$ and $s_{1/2}$ strength observed in this experiment. From Table III, one can see that only 35% of the $2d_{5/2}$ strength is accounted for in the $2p_{1/2}$ IAS decay and a very small amount for the other IAS. On the contrary, the occupancy of the $3s_{1/2}$ orbital in ^{96}Zr deduced from our results (20 to 40%) is rather large as compared to the values obtained from neutron pickup experiment on the same target (2 to 5%).⁵ This result could be explained by the large uncertainties on the C^2S number deduced for the badly matched $l=0$ transition in the study of the $^{96}\text{Zr}(^3\text{He}, \alpha)^{95}\text{Zr}$ reaction.⁵ In the case of the $l=2$ missing strength a number of levels in ^{94}Y might not have been observed due to their very low proton branching ratios.

SUMMARY

We have presented in this paper a rather comprehensive study of the reactions $^{96}\text{Zr}(^3\text{He}, \alpha\bar{p})$ and $^{144}\text{Sm}(^3\text{He}, \alpha\bar{p})$ on hole analog states. This work is the first experimental attempt to study the decay of $T_{>}$ hole states in heavy nuclei and consequently we have developed the implication of this study on our knowledge about hole-hole multiplets in odd-odd heavy nuclei. Comparisons have been made between the selective population of such levels in the $(^3\text{He}, \alpha\bar{p})$ process and the study of neutron-particle-hole states of the target in the well known IAR experiments.

We wish to emphasize that the study of the proton decay of hole analog states investigated using the $(^3\text{He}, \alpha\bar{p})$ process in a suitable geometry is almost a unique way to obtain quantitative results for the

configurations of nuclear levels in odd-odd nuclei. Moreover, a knowledge of such wave functions in the analysis of the (d, α) or $(p, {}^3\text{He})$ reactions leading to the same residual states could be of use in obtaining a normalization factor in theoretical analysis of such two nucleon transfer reactions.

We wish to thank Dr. N. M. Rao and E. Hourani for their help in the last stage of this work. We acknowledge L. Stab for the fabrication of the Si(Li) detectors and the operating crew of the Orsay tandem Van de Graaff for the efficient running of the accelerator.

¹G. M. Temmer, in *Isospin in Nuclear Physics*, edited by D. H. Wilkinson (North-Holland, Amsterdam, 1969), p. 695, and references therein.

²R. L. Kozub and D. H. Youngblood, *Phys. Rev. C* **7**, 410 (1973).

³M. Sekiguchi, Y. Shida, F. Soga, Y. Hirao, and M. Sakai, *Nucl. Phys.* **A278**, 231 (1977).

⁴G. Berrier-Ronsin, G. Duhamel, S. Galès, E. Gerlic, E. Hourani, H. Langevin-Joliot, J. Van de Wiele, and M. Vergnes, in *Proceedings of the International Conference on Nuclear Structure*, Tokyo, 1977 (unpublished), p. 343.

⁵S. Galès, E. Hourani, S. Fortier, H. Laurent, J. M. Maison, and J. P. Schapira, *Nucl. Phys.* **A288**, 201 (1977).

⁶S. Galès, S. Fortier, H. Laurent, J. M. Maison, and

J. P. Schapira, *Nucl. Phys.* **A259**, 189 (1976); *Phys. Rev. C* **14**, 842 (1976).

⁷H. Laurent, J. P. Schapira, S. Fortier, S. Galès, and J. M. Maison, *Nucl. Instrum. Methods* **117**, 17 (1974).

⁸B. H. Wildenthal, E. Newman, and R. L. Auble, *Phys. Rev. C* **3**, 1199 (1971).

⁹A. E. Litherland and A. J. Ferguson, *Can. J. Phys.* **39**, 788 (1961).

¹⁰J. F. Lemming and S. Raman, *Nucl. Data* **B10**, 309 (1973).

¹¹R. Martin *et al.*, *Nucl. Phys.* **A210**, 221 (1973).

¹²S. Gilad *et al.*, *Nucl. Phys.* **A233**, 81 (1974).

¹³D. C. Kocher, *Nucl. Data* **B10**, 241 (1973).

¹⁴W. R. Coker and G. W. Hoffmann, *Z. Phys.* **263**, 179 (1973).